Reactive & Functional Polymers 71 (2011) 140–147

Contents lists available at ScienceDirect

Reactive & Functional Polymers

journal homepage: www.elsevier.com/locate/react

Intramolecular charge transfer induced by deprotonation of hydroxyl groups in π-conjugated polymers with π-deficient aromatic rings

Isao Yamaguchi *, Hidehito Mitsuno

Department of Material Science, Faculty of Science and Engineering, Shimane University, 1060 Nishikawatsu, Matsue 690-8504, Japan

ARTICLE INFO

Article history:
Received 10 September 2010
Received in revised form 8 November 2010
Accepted 8 November 2010
Available online 20 November 2010

Keywords:
Intramolecular charge transfer
Conjugated polymer
Triazole
Oxadiazole

ABSTRACT

π-Conjugated polymers consisting of *p*-phenylene (Ph) and 1,3,4-oxadiazole (Oz) or 4-octylphenyl-1,3,4-triazole (OctOz) rings [*polymer-1*: $(Ph\text{-}Oz)_n$ and *polymer-2*: $(Ph\text{-}OctTz)_n$] and those consisting of 9,9-dihexyl-2,7-fluorene (Flu) and Oz or 1-(4-hydroxyphenyl)-1,3,4-triazole (HOPhTz) rings [*polymer-3*: $(Ph\text{-}Oz\text{-}Py\text{-}Oz\text{-}Flu)_n$ and *polymer-4*: $(Ph\text{-}HOPhTz\text{-}Py\text{-}HOPhTz\text{-}Flu)_n$ (Py = 2,5-pyridine)] were synthesized by polymerization promoted by polyphospholic acid and catalyzed by a Pd complex, respectively. Model compounds (*model-1*: Ph-Oz-Py-Oz-Ph, *model-2*: Ph-HOPhTz-Py-HOPhTz-Ph, and *model-3*: Ph-OctPhTz-Py-OctPhTz-Ph) were synthesized. The fact that the λ_{max} wavelengths of the polymers were longer than those of the model compounds suggests the expansion of the π-conjugation system along the polymer chain. The reaction of *polymer-4* and *model-2* with NaH caused the dehydration of the OH groups, which induced an intramolecular charge transfer (ICT) from the ONa group to the Tz ring. The ICT affected the optical properties of the polymers and the model compounds. The cast films of polymers obtained in this study underwent electrochemical reduction and oxidation.

1. Introduction

Charge transfer (CT) type π-conjugated polymers have received much attention because of their potential use as materials for photovoltaic and electroluminescence devices [1–11]. Intramolecular CT (ICT) in π-conjugated polymers significantly affects their optical and electric properties; it can be caused by stimulating the polymers with photo irradiation or heating [8]. π-Conjugated polymers that consist of either π-excess or π-deficient aromatic rings have been reported to cause ICT [4]. Thus, the introduction of a site that sensitizes external stimuli to cause ICT and the formation of both π-excess and π-deficient aromatic rings in π-conjugated polymers is a promising approach for the development of new CT-type materials.

Recently, polyphenoles with oligo(*p*-phenylene) pendant groups and their significant solvatochromism after the deprotonation of the OH group for the polymers with NaH were reported [12]. In other words, the emission color of the deprotonated polymers can be tuned by solvents. The wavelength at which the emission peak was observed shifted to a longer wavelength with an increase in the donor number (DN) of the solvents. These phenomena were attributed to ICT from the ONa group to the adjacent benzene rings. ICT from the ONa group to the π-deficient aromatic ring should occur more easily than that from the ONa group to the benzene ring. According to this assumption, π-conjugated polymers with a sodium phenolato pendant group at the π-deficient aromatic ring show a smooth ICT from the ONa group to the π-deficient aromatic ring. Investigating the chemical properties of such π-conjugated polymers can provide fundamental information for the development of new emitting materials. In this study, triazole was used as a π-deficient aromatic ring because of its high electron affinity, thermal stability, and facile *N*-substitution. π-Conjugated polymers with π-deficient aromatic rings such as triazole and oxadiazole have received considerable attention because of their strong blue emission and high thermal stability [10,13–19]. However, to the best of our knowledge, there has been no research on π-conjugated polymers that shows ICT caused by the reaction of the polymers with NaH. In this study, π-conjugated polymers consisting of 9,9-dihexyl-2,7-fluorene groups and 1,3,4-oxadiazole (Oz) or 4-hydroxyphenyl-1,3,4-triazole (HOPh-Tz) rings, which generate an electron-donating ONa group through treatment with a base, were synthesized. The triazole ring located between two benzene rings at the 2,5-positions has been reported to be orthogonal to them [20], which reduces the steric crowding between the phenylene rings attached to triazole and effectively limits the π-conjugation range. In this study, to obtain polymers with a long π-conjugation system, a 2,5-pyridine (Py) ring was placed between the Oz and Tz rings in the polymer main chain. The Py ring can reduce the steric crowding with the Oz and Tz rings because the number of *o*-H atoms in the Py ring is less than that in the *p*-phenylene ring.

* Corresponding author.
E-mail address: iyamaguchi@riko.shimane-u.ac.jp (I. Yamaguchi).

1381-5148/$ - see front matter © 2010 Elsevier Ltd. All rights reserved.
doi:10.1016/j.reactfunctpolym.2010.11.014

The synthesis and optical, electrochemical, and thermal properties of CT-type π-conjugated polymers with π-deficient Tz or Oz rings and the corresponding model compounds are reported.

2. Experimental

2.1. General

Solvents were dried, distilled, and stored under nitrogen. Subsequently, **1**, **2**, and **3** were synthesized according to the literature [21]. Other reagents were purchased and used without further purification. Reactions were carried out with standard Schlenk techniques under nitrogen.

IR and NMR spectra were recorded on a JASCO FT/IR-660 PLUS spectrophotometer with a KBr pellet and a JEOL AL-400 spectrometer, respectively. Elemental analysis was conducted on a Yanagimoto MT-5 CHN corder. UV–vis and PL spectra were obtained by a JASCO V-560 spectrometer and a JASCO FP-6200, respectively. Quantum yields were calculated by using a diluted ethanol solution of 7-dimethylamino-4-methylcoumarin as the standard. Cyclic voltammetry was performed in a DMSO solution containing 0.10 M $[Et_4N]BF_4$ with a Hokuto Denko HSV-110. Pt plate and Ag wire were used as working and counter electrodes and reference electrode, respectively. TGA curves were obtained by a Rigaku Thermo plus TG8120. The ground-state geometries of model compounds were optimized with the Gaussian 09 computer program at the density functional theory (DFT) level using the B3LYP/6-31G* functional [22].

2.2. Synthesis of monomer-1

1 (0.11 g, 0.20 mmol) was dissolved in polyphospholic acid (PPA) (20 mL) at 140 °C. After the solution was stirred at that temperature for 72 h, it was poured in water (300 mL). The resulting precipitate was collected by filtration, washed with water and methanol, and dissolved in DMSO at 100 °C. When the DMSO solution was cooled to room temperature, a gray solid was precipitated from the solution. The precipitate was collected by filtration, washed with methanol, and dried under vacuum to obtain *monomer-1* as a white powder (0.077 g, 73%). ^{1}H NMR (400 MHz, $CDCl_3$): δ 9.47 (s, 1H), 8.72 (d, J = 6.8 Hz, 1H), 8.47 (d, J = 8.4 Hz, 1H), 8.06–8.11 (m, 4H), 7.84 (d, J = 8.0 Hz, 4H). ^{13}C NMR (100 MHz, $CDCl_3$): δ 155.3, 144.3, 141.6, 140.1, 138.9, 135.2, 131.8, 131.3, 130.1, 128.5, 128.2, 124.3, 122.6, 122.3, 109.5. Calcd for $C_{21}H_{11}N_5Br_2O_2{\cdot}0.5H_2O$: C, 47.22; H, 2.26; N, 13.11. Found: C, 47.20; H, 2.65; N, 12.75.

2.3. Synthesis of model-1

Model-1 was synthesized using a procedure similar to that used for *monomer-1*. ^{1}H NMR (400 MHz, DMSO-d_6): δ 9.54 (s, 1H), 8.78 (dd, J = 2.0 Hz and 8.0 Hz, 1H), 8.53 (d, J = 8.4 Hz, 1H), 8.19 (dd, J = 6.0 Hz and 9.2 Hz, 4H), 7.66–7.69 (m, 6H). ^{13}C NMR (100 MHz, DMSO-d_6): δ 165.3, 146.6, 136.7, 136.1, 132.3, 129.5, 128.8, 128.1, 127.8, 127.1, 125.7, 125.5, 123.9, 123.4, 123.2, 122.6, 122.3, 121.1, 119.7, 118.9, 117.4. Calcd for $C_{21}H_{13}N_5O_2{\cdot}0.5H_2O$: C, 67.02; H, 3.75; N, 18.61. Found; C, 66.89; H, 4.01; N, 18.25.

2.4. Synthesis of monomer-2

$CaCl_2$ (2.0 g, 18.0 mmol) was added to an NMP (30 mL) solution of *monomer-1* (1.1 g, 2.1 mmol) and *p*-anisidine (3.7 g, 30 mmol). After the reaction mixture was stirred at 175 °C for 96 h, the solvent was removed under vacuum. The resulting solid was dissolved in methanol (30 mL) and the solution was refluxed for 72 h. The precipitate from the solution was washed with methanol, collected by filtration, and dried under vacuum to obtain *monomer-2* as a white powder (1.3 g, 86%). ^{1}H NMR (400 MHz, DMSO-d_6): δ 10.1 (s, 1H), 9.89 (s, 1H), 8.44 (s, 1H), 7.95 (d, J = 8.4 Hz, 1H), 7.83 (dd, J = 2.0 Hz and 8.4 Hz, 1H), 7.60–7.63 (m, 4H), 7.35 (d, J = 8.0 Hz, 4H), 7.26 (d, J = 8.4 Hz, 2H), 7.15 (d, J = 8.4 Hz, 2H), 6.82 (d, J = 8.8 Hz, 2H), 6.74 (d, J = 8.4 Hz, 2H). ^{13}C NMR (100 MHz, DMSO-d_6): δ 159.3, 158.0, 154.3, 152.1, 150.0, 148.0, 145.3, 131.6, 130.3, 129.3, 129.2, 126.6, 126.1, 125.9, 125.3, 123.5, 118.7, 117.8, 116.7, 116.7, 116.5, 115.9, 115.7, 115.0, 114.5, 111.3. Calcd for $C_{33}H_{21}N_7Br_2O_2{\cdot}0.4H_2O$: C, 56.03; H, 2.99; N, 13.86. Found; C, 55.77; H, 3.22; N, 13.42.

2.5. Synthesis of model-2

Model-2 was synthesized using a procedure similar to that used for *monomer-2*. ^{1}H NMR (400 MHz, DMSO-d_6): δ 10.1 (s, 1H), 9.85 (s, 1H), 8.45 (s, 1H), 7.95 (d, J = 8.0 Hz, 1H), 7.83 (dd, J = 2.4 Hz and 8.0 Hz, 1H), 7.39–7.42 (m, 10H), 7.25 (d, J = 8.8 Hz, 2H), 7.14 (d, J = 8.8 Hz, 2H), 6.82 (d, J = 8.8 Hz, 2H), 6.74 (d, J = 8.8 Hz, 2H). ^{13}C NMR (100 MHz, DMSO-d_6): δ 158.4, 157.8, 154.9, 153.1, 151.9, 148.0, 147.2, 136.3, 129.7, 129.4, 129.3, 128.4, 126.9, 126.1, 125.2, 123.7, 116.4, 115.6. Calcd for $C_{33}H_{23}N_7O_2{\cdot}0.3H_2O$: C, 71.42; H, 4.29; N, 17.67. Found; C, 71.50; H, 4.11; N, 17.39.

2.6. Synthesis of model-3

Model-3 was synthesized using a procedure similar to that used for *monomer-1*. ^{1}H NMR (400 MHz, DMSO-d_6): δ 8.51 (s, 8H),8.24 (d, J = 7.6 Hz, 4H), 7.82 (d, J = 7.6 Hz, 2H), 7.70 (t, J = 8.0 Hz, 4H), 7.30 (s, 4H), 2.64 (t, J = 8.0 Hz, 4H), 1.61 (t, J = 8.0 Hz, 4H), 1.24–1.30 (m, 20H), 0.83 (t, J = 7.2 Hz, 6H). ^{13}C NMR (100 MHz, DMSO-d6): δ169.2, 166.8, 149.3, 138.9, 132.9, 132.7, 132.5, 131.1, 130.7, 127.8, 122.2, 120.3. Calcd for $C_{33}H_{23}N_7O_2{\cdot}0.6H_2O$: C, 70.73; H, 4.35; N, 17.50. Found; C, 70.90; H, 4.60; N, 17.88.

2.7. Synthesis of polymer-1

Terephthaloyl chloride (1.0 g, 5.0 mmol) was added to an NMP solution (100 mL) of terephthalic dihydrazide (0.97 g, 5.0 mmol) by portions over 2 h in an ice bath. The reaction solution was stirred at 0 °C for 2 h and at room temperature for 50 h and was poured in water (500 mL). The resulting precipitate was washed with acetone (200 mL) two times, collected by filtration, and dried under vacuum to obtain a precursor polymer (1.61 g, 100%). The precursor polymer (0.81 g, 2.5 mmol) was dissolved in PPA (100 mL). The reaction solution was stirred at 175 °C for 72 h and poured in water (500 mL). The resulting precipitate was washed with methanol (300 mL) and dried under vacuum to obtain *polymer-1* as a light brown powder (0.39 g, 54%). ^{1}H NMR (400 MHz, D_2SO_4): δ 8.80. Calcd for $C_{16}H_8N_4O_2{\cdot}0.5H_2O$: C, 64.65; H, 3.05; N, 18.85. Found; C, 64.48; H, 3.18; N, 18.64.

2.8. Synthesis of polymer-2

A mixture of *polymer-1* (0.32 g, 1.1 mmol) and 4-octylaniline (1.3 g, 10 mmol) was stirred at 170 °C for 72 h and poured in water (500 mL). The resulting precipitate was washed with methanol (300 mL) two times, collected by filtration, and dried under vacuum to obtain *polymer-2* as a light brown powder (0.47 g, 64%). ^{1}H NMR (400 MHz, D_2SO_4): δ 9.31 (4H), 7.94–8.54 (4H). Calcd for $C_{44}H_{50}N_6$: C, 79.72; H, 7.69; N, 12.68. Found: C, 78.99; H, 7.00; N, 12.15.

2.9. Synthesis of polymer-3

Monomer-1 (0.26 g, 0.50 mmol) and 9,9-dihexyl-2,7-diboronic acid trimethylene ester (0.25 g, 0.50 mmol) were dissolved in 20 mL of dry NMP under N_2. To the solution were added K_2CO_3(aq) (2.0 M, 4 mL; N_2 bubbled before use) and $Pd(PPh_3)_4$ (0.058 g, 0.050 mmol). After the mixture was stirred for 72 h at 100 °C, the solvent was removed under vacuum. The resulting solid was washed with water and acetone. *Polymer-3* was collected by filtration, dried under vacuum, and obtained as a light brown powder (0.34 g, 97%). ^{1}H NMR (400 MHz, DMSO-d_6): δ 7.71–8.34 (17H), 2.13 (4H), 1.07 (12H), 0.74 (10H). Calcd for $C_{46}H_{43}N_5O_2{\cdot}0.5H_2O$: C, 78.16; H, 6.27; N, 9.91. Found: C, 77.84; H, 6.15; N, 10.09.

2.10. Synthesis of polymer-4

Polymer-4 was synthesized using a procedure similar to that used for *polymer-3*.

^{1}H NMR (400 MHz, DMSO-d_6): δ 8.49 (1H), 7.66–7.90 (14H), 7.08–7.16 (5H), 6.78–6.85 (5H), 2.12 (4H), 1.06 (12H), 0.74 (10H). Calcd for $C_{58}H_{53}N_7O_2{\cdot}H_2O$: C, 77.57; H, 6.17; N, 10.92. Found: C, 77.90; H, 5.89; N, 10.61.

3. Results and discussion

3.1. Synthesis

The reaction of 4-bromobenzoyl chloride and benzoyl chloride with 2,5-pyridine dihydrazide at a 2:1 molar ratio followed by treatment with thionyl chloride yielded *nonomer-1* and *model-1*, respectively (Scheme 1a and b). The reaction of *nonomer-1* and *model-1* with *p*-anisidine in the presence of $CaCl_2$ caused the transformation from the oxadiazole ring to the triazole ring accompanied by hydrolysis of the OCH_3 group to yield *monomer-2* and *model-2*, respectively (Scheme 1c). The reaction **3** with *p*-octylaniline at a 1:2 molar ratio in the presence of PPA yielded *model-3* (Scheme 1d). These synthesis results are summarized in Table 1.

The polymerization of terephthaloyl chloride with 1,4-benzene dihydrazide followed by treatment with PPA yielded *polymer-1*

Table 1
Synthesis results and optical properties.

	Yield, %	η_{sp}/c, dL g^{-1}	Absorption, nm		PL, nm
			In solution	In film	
Monomer-1	86	–	–	–	–
Monomer-2	86	–	–	–	–
Model-1	87	–	325[c]	–	410[c]
Model-2	79	–	308[c]	–	390[c]
Model-3	65	–	324[c]	–	349, 368, 387[c]
Polymer-1	54	–	346[d]	–	407[d]
Polymer-2	64	2.02[a]	347[d]	364, 380[f]	407[d]
Polymer-3	97	1.24[b]	345[e]	–	407 (408) [g]
Polymer-4	93	1.71[b]	357 (357)[e]	359	407 (542) [g]

[a] In conc. H_2SO_4 at 30 °C (c = 0.10 g dL^{-1}).
[b] In NMP at 30 °C (c = 0.10 g dL^{-1}).
[c] In NMP.
[d] In conc. H_2SO_4.
[e] In NMP. λ_{max} value after treatment with NaH was shown in parenthesis.
[f] Shoulder peak.
[g] In NMP. λ_{em} value after treatment with NaH was shown in parenthesis.

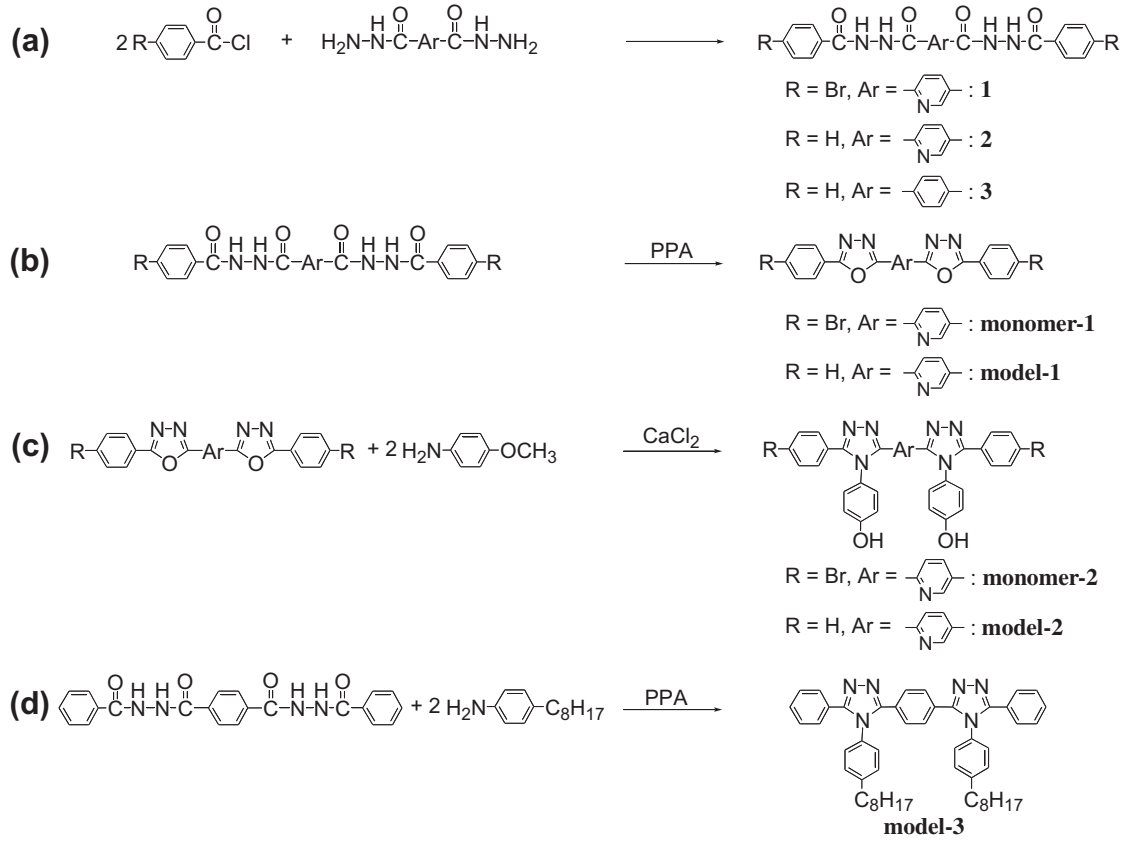

Scheme 1. Synthesis of monomers and model compounds.

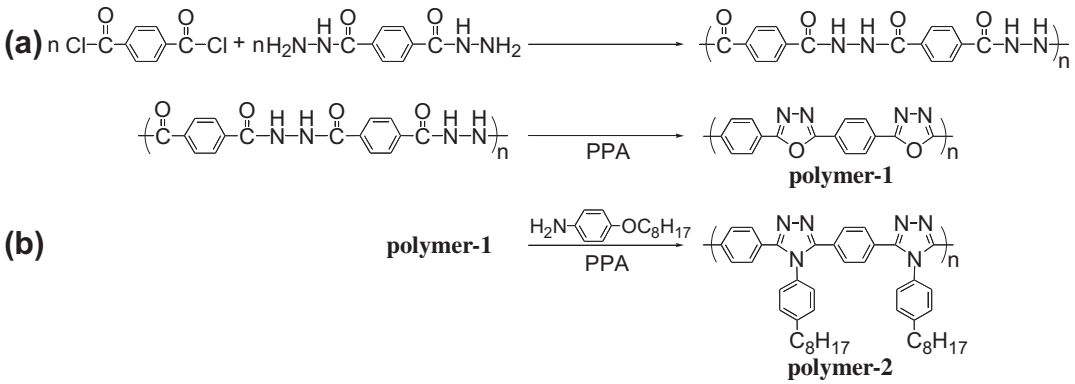

Scheme 2. Synthesis of polymers consisted of *p*-phenylene and oxadiazole or triazole rings.

Table 2
Solubility of monomers, model compounds, and polymers[a].

	$CHCl_3$	DMF	DMSO	NMP	CF_3COOH	H_2SO_4
Monomer-1	–	++	++	++	++	++
Monomer-2	–	++	++	++	++	++
Model-1	++	++	++	++	++	++
Model-2	–	++	++	++	++	++
Model-3	–	–	–	–	++	++
Polymer-1	–	–	–	–	–	++
Polymer-2	–	–	–	–	++	++
Polymer-3	–	++	++	++	–	++
Polymer-4	–	+	+	++	++	++

[a] ++: soluble, +: partly soluble, –: insoluble.

(Scheme 2a). The reaction of *polymer-1* with 4-octylaniline caused the conversion from the Oz ring to the Tz ring to yield *polymer-2* (Scheme 2b). The conversion of the oxazole rings in *monomer-1*, *model-1*, and *polymer-1* to the triazole rings in *monomer-2*, *model-2*, and *polymer-2* requires an excess amount of amine because of the low reaction efficiency. The solubilities of the obtained monomers, model compounds, and polymers are summarized in Table 2. *Polymer-1* and *polymer-2* were soluble in acidic solvents such as trifluoroacetic acid and sulfuric acid but insoluble in organic solvents.

To obtain polymers soluble in non-acidic organic solvents, the Pd-complex-catalyzed polymerization of *monomer-1* and *monomer-2* with 9,9-dihexyl-2,7-diboronic acid trimethylene ester was carried out and resulted in yields of 97% and 93% for *polymer-3* and *polymer-4*, respectively (Scheme 3). *Polymer-3* was completely soluble in polar organic solvents such as *N*,*N*-dimethylformamide (DMF), dimethyl sulfoxide (DMSO), and *N*-methyl-2-pyrollidone (NMP), whereas *polymer-4* was partly soluble in these solvents.

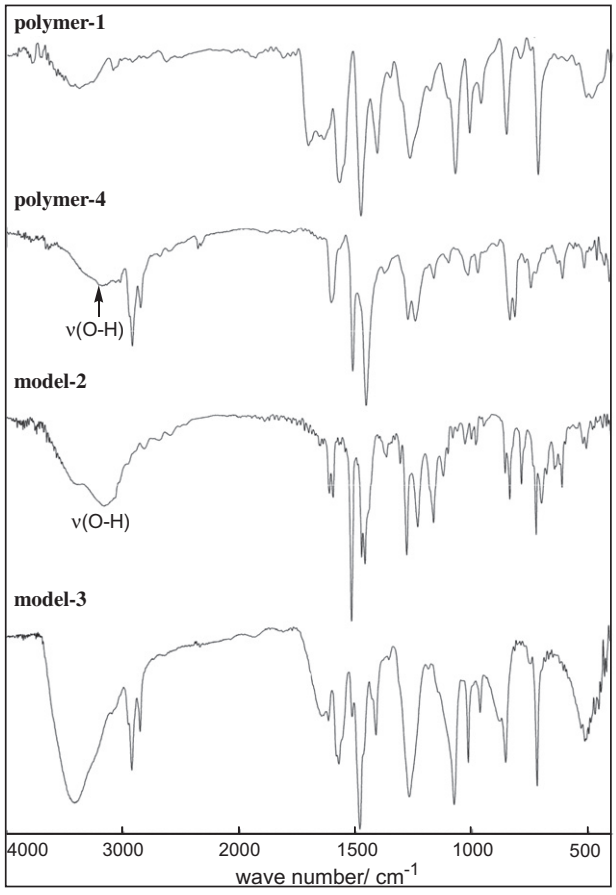

Fig. 1. IR spectra of *polymer-1*, *polymer-4*, *model-2*, and *model-3*.

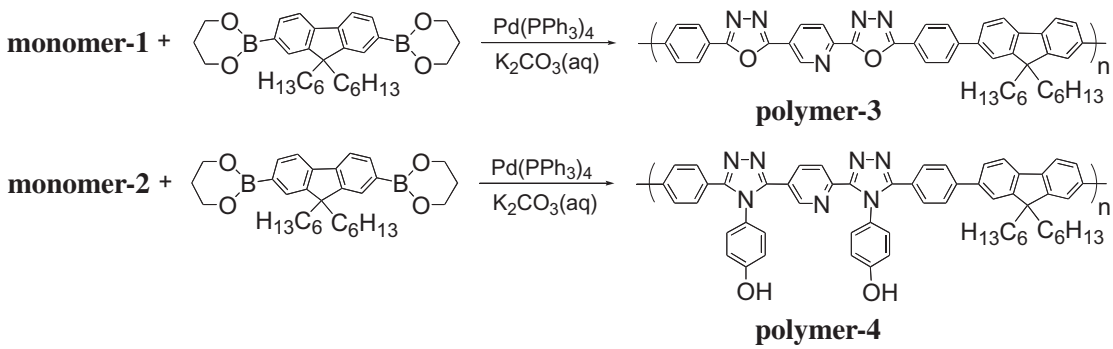

Scheme 3. Synthesis of polymers with 9,9-dihexyl-2,7-fluorene and oxadiazole or triazole rings.

The intrinsic viscosities for a sulfuric acid solution of *polymer-2* and NMP solutions of *polymer-3* and *polymer-4* at a concentration of 0.10 g dL^{-1} were 2.02, 1.24, and 1.71 dL g^{-1}, respectively. GPC measurements could not be carried out because of the low solubilities of the polymers in the eluent.

3.2. IR and NMR spectra

Fig. 1 depicts the IR spectra of *polymer-1*, *polymer-4*, *model-2*, and *model-3*. The disappearance of the peak corresponding to ν(C═O) in the IR spectra of *polymer-1* and *model-3* suggests that the triazole ring formation reaction proceeded to completion. The IR spectrum of *polymer-4* resembles that of *model-2*. The broad absorption at around 3100 cm^{-1} was assigned to ν(O—H) of the hydrogen bonding OH groups in *polymer-4* and *model-2*.

Fig. 2 depicts the ^{1}H NMR spectra of *polymer-1*, *polymer-2*, and *model-3* in CF_3COOD. The peak assignments are indicated in the figure. The peaks corresponding to the protons of the benzene rings at the 2,5-positions of the triazole ring in *polymer-2* were observed at higher magnetic field positions than in *polymer-1*. Thus, the electron negativity of the triazole ring is lower than that of the oxadiazole ring [23]. The peaks corresponding to the protons of the benzene rings and hexyl groups in *polymer-2* were observed at almost the same positions as those in *model-3*.

Fig. 3 depicts the ^{1}H NMR spectra of *model-2* and *polymer-4* before and after the deprotonation of the OH groups with NaH in DMSO-d_6. The peak integral between the aromatic and aliphatic protons supports the structures of the polymer and model compound. The peaks corresponding to the OH groups of *model-2* disappeared after treatment with NaH, suggesting that the deprotonation proceeded to completion. The benzene and pyridine protons in *model-2* shifted to high magnetic field positions after the deprotonation because of the generation of electron-donating ONa groups. The peak shifts of the *p*-phenylene protons were larger than those of the pyridine protons because the phenylene rings are close to the ONa group. The peak corresponding to the OH protons of *polymer-4* was not observed in the ^{1}H NMR spectrum. The reason for the disappearance is unclear. However, the peaks corresponding to the benzene and pyridine protons in *polymer-4* shifted to high magnetic field positions after treatment with NaH because of the generation of the electron-donating ONa groups, as shown in Fig. 3b. These results support the presence of OH groups in *polymer-4*. Additionally, the presence of OH groups in *polymer-4* is supported by the fact that IR absorption that can be assigned to ν(O—H) of *model-2* and *polymer-4* was observed at the same wave number, as mentioned above.

3.3. UV–vis and PL spectra

Fig. 4 depicts the UV–vis spectra of *model-2* and *polymer-4* in *N*-methyl-2-pyrrolidone (NMP) before and after the addition of an excess amount of NaH. The wavelength at which the absorption maximum (λ_{max}) for *polymer-4* was observed was longer than that of *model-2*, suggesting that the π-conjugation system of *polymer-4* expanded along the polymer chain. The λ_{max} values for *model-2* and *polymer-4* barely changed after the deprotonation of the OH groups. However, new broad absorptions appeared in the ranges of 370–430 and 400–480 nm in the UV–vis spectra for *model-3* and *polymer-4*, respectively.

The λ_{max} value for the NMP solution of *polymer-4* was larger than that for the sulfuric acid solution of *polymer-2*. These observations correspond to the smaller number of *o*-protons in the 2,5-pyridine ring, which reduced the twisting of the polymer chain. However, the λ_{max} value for the cast film of *polymer-2* (364 nm) was larger than that for *polymer-4* (359 nm). These observations correspond to the assumption that *polymer-2* forms a π-stacked structure in film. The fact that the powder X-ray diffraction

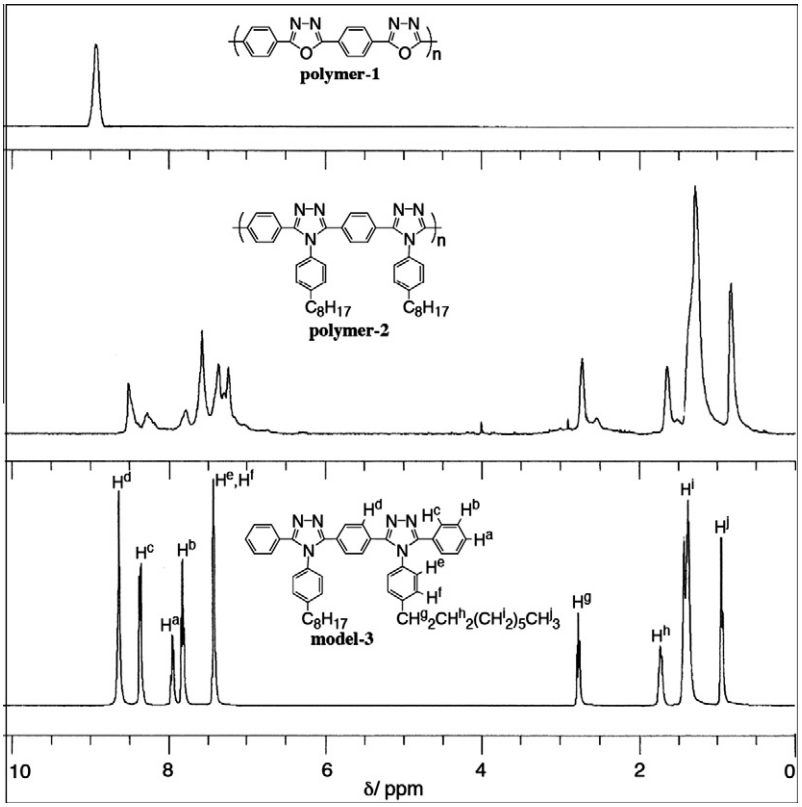

Fig. 2. ^{1}H NMR spectra of *polymer-1*, *polymer-2*, and *model-3* in CF_3COOD.

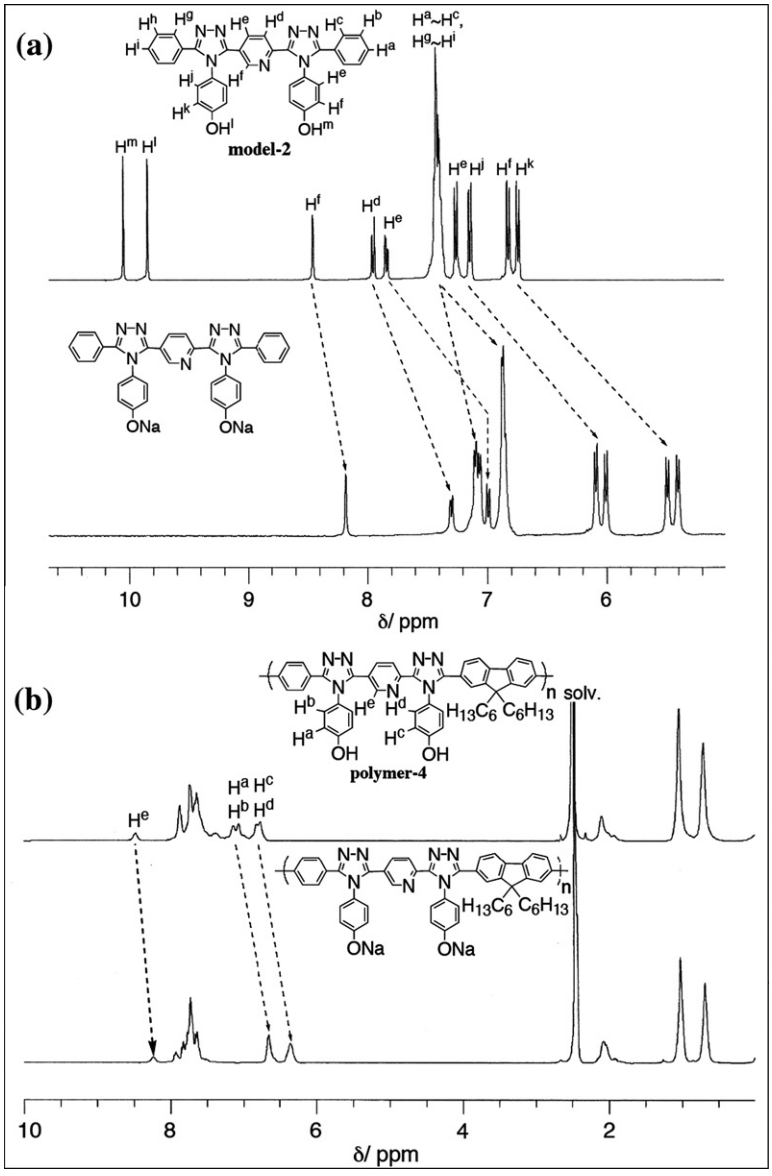

Fig. 3. ^{1}H NMR spectra of *model-2* and *polymer-4* before and after the deprotonation of the OH groups with NaH in DMSO-d_6.

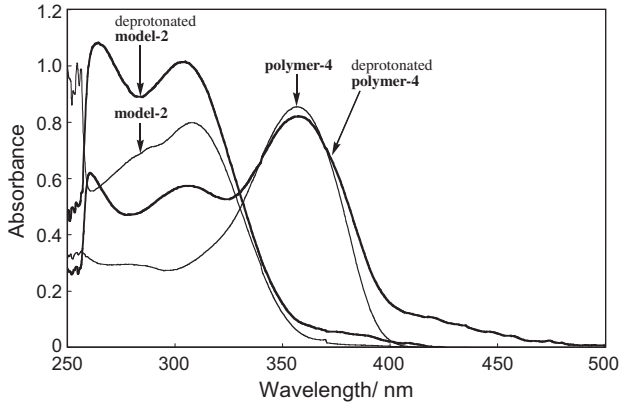

Fig. 4. UV–vis spectra of *model-2* and *polymer-4* in NMP before and after the addition of an excess amount of NaH.

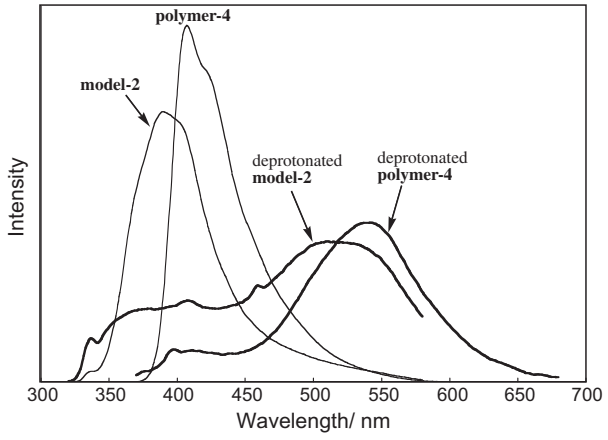

Fig. 5. PL spectra of *model-2* and *polymer-4* in NMP before and after the addition of an excess amount of NaH.

(XRD) pattern of *polymer-2* showed peaks at 8.6° and 21.3° in contrast to the broad XRD pattern of *polymer-4* supports the occurrence of π-stacking for *polymer-2* in film. Rigid π-conjugated polymers with long alkyl side chains have been reported to form

π-stacked structures, which causes a bathochromic shift of λ_{max} [24–30].

Fig. 5 depicts the photoluminescence (PL) spectra of *model-2* and *polymer-4* in *N*-methyl-2-pyrrolidone (NMP) before and after the addition of an excess amount of NaH. The PL peak positions of *model-2* and *polymer-4* in NMP shifted to longer wavelengths with the deprotonation of the OH groups. The degrees of bathochromic shift ($\Delta\lambda_{em}$) in the PL peak positions for *model-2* and *polymer-4* were 125 and 135 nm, respectively. The λ_{em} position of polyphenylene with the hydroxy[1,1′;4′,1″]terphenyl unit (*polymer-5(OH)*) has been reported to shift by 110 nm to a longer wavelength after the deprotonation of the OH group in DMF [12].

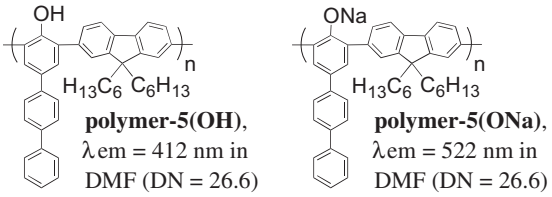

The fact that the $\Delta\lambda_{em}$ value in *polymer-4* was larger than that in *polymer-5* ($\Delta\lambda_{em}$ = 110 nm) apparently corresponds to the assumption that the charge transfer from the ONa group to the electron-accepting triazole ring occurs more easily than that from the ONa group to the adjacent benzene rings. The PL peak position of *polymer-3* (408 nm) was essentially the same as that of *polymer-4* (407 nm). However, the PL peak position of *polymer-3* was almost unchanged by the treatment with NaH. This result confirms that the bathochromic shift in the PL peak position of *polymer-4* after treatment with NaH can be attributed to the formation of the ONa group. The PL intensities of *model-2* (Φ = 0.004) and *polymer-4* (Φ = 0.006) after deprotonation were considerably lower than those of *model-2* (Φ = 0.21) and *polymer-4* (Φ = 0.35) before deprotonation because of the ICT in the deprotonated species. ICT in π-conjugated polymers has been reported to reduce their PL emission efficiencies [31].

3.4. Computational calculations

To obtain information on the ICT in *model-2* and *polymer-4* after deprotonation of the OH groups, the molecular orbitals of *model-4(OH)* and *model-4(ONa)* were compared with computational calculations at the density functional theory (DFT) level. *Model-4(OH)* and *model-4(ONa)* with symmetric structures are suitable for rapid calculations.

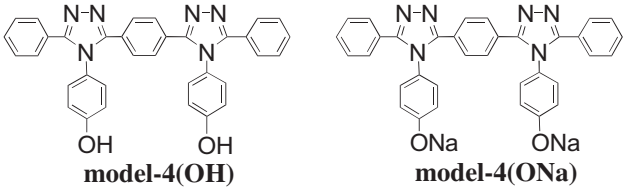

Fig. S1 shows the calculated HOMOs of *model-4(OH)* and *model-4(ONa)*. In the case of *model-4(ONa)*, there are distributed electrons between the triazole ring and the phenolate ring. In contrast, there are no distributed electrons between the triazole ring and the phenolate ring in *model-4(OH)*. These observations support the assumption that ICT between the phenolate ring and the triazole ring occurred in the deprotonated species.

3.5. Cyclic voltammograms

Fig. 6 depicts cyclic voltammograms for the cast films of *polymer-3* and *polymer-4*. *Polymer-3* showed an anodic peak at 1.68 V

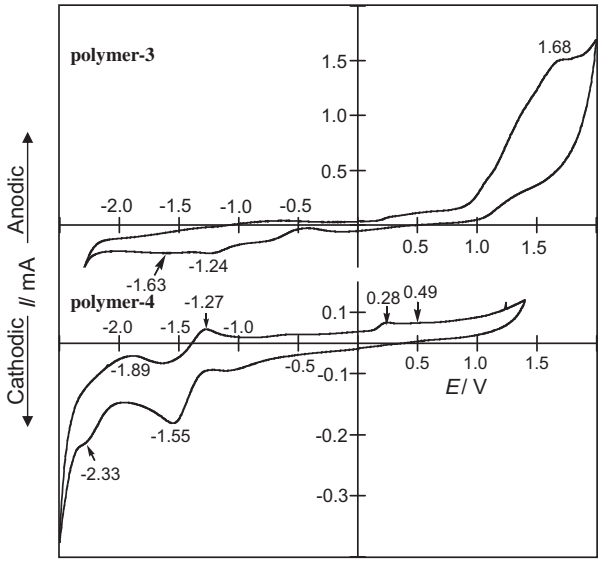

Fig. 6. Cyclic voltammograms for the cast films of *polymer-3* and *polymer-4* in an acetonitrile solution (0.10 M) of $[Et_4N]BF_4$. The scan rate was 50 mV s^{-1}.

vs. Ag^+/Ag corresponding to the electrochemical oxidation of the 2,7-diphenylfluorene unit. However, the corresponding reduction (p-dedoping) peak did not appear in the cyclic voltammograms, likely because of the formation of a stable adduct between the electrochemically oxidized polymer and BF_4^-. Electrochemically oxidized π-conjugated polymers have been reported to form stable adducts with BF_4^- during cyclic voltammetry measurements [32]. The electrochemical reaction was accompanied by electrochromism. The yellow cast film of the polymer changed to reddish brown after electrochemical oxidation. The cyclic voltammogram of *polymer-3* showed two peaks at –1.24 and –1.63 V vs. Ag^+/Ag corresponding to the electrochemical reduction of the oxadiazole and pyridine rings, respectively. As depicted in Fig. 6b, two peaks corresponding to the electrochemical oxidation of the two OH groups in *polymer-4* were observed at 0.28 and 0.49 V vs. Ag^+/Ag. The cyclic voltammogram of *polymer-4* showed two peaks at –1.55 and –2.23 V vs. Ag^+/Ag corresponding to the electrochemical reduction of the triazole and pyridine rings, respectively, which were coupled with the peaks at –1.27 and -1.89 V vs. Ag^+/Ag, respectively. The results show that the cathodic potential of the peak corresponding to the electrochemical reduction of the pyridine ring of *polymer-4* was higher than that of *polymer-3* due to the lower electronic negativity of the triazole ring compared to the oxadiazole ring.

3.6. Thermal properties

Fig. S2 shows TGA curves of *polymer-3* and *polymer-4*. The weight loss of the polymers in the range of 80–300 °C corresponds to the thermal loss of hydrated water in the polymers. *Polymer-4* started a gradual weight loss due to the thermal decomposition of the polymer chain at 300 °C and 95% weight of the polymer caused thermal decomposition at 600 °C. In contrast, *polymer-3* showed a high thermal stability. Approximately 50% of the weight of the polymer remained at 600 °C. The higher thermal stability of *polymer-3* appeared to be due to its rigid structure.

4. Conclusion

π-Conjugated polymers with Oz and HOPhTz groups were obtained by polymerization promoted by polyphospholic acid and

catalyzed by a Pd complex. The expansion of the π-conjugation system of the polymers along the polymer chain was confirmed by the results showing that the λ_{max} wavelengths of the polymers were longer than those of the corresponding model compounds. The reaction of the polymer with HOPhTz groups with NaH caused the deprotonation of the OH groups, which led to ICT from the ONa group to the Tz ring. The ICT affected the optical properties of the polymer. The absorption and PL peak positions of the deprotonated polymer shifted toward longer wavelengths compared with the polymer before deprotonation. The cast films of the polymers obtained in this study underwent electrochemical reduction and oxidation. The results obtained in this study indicate that the ICT caused by the deprotonation of an OH group with a base in π-conjugated polymers is a useful phenomenon for the development of new functional materials.

Acknowledgment

The authors wish to thank Dr. H. Shiratori in their department for help with DFT measurements.

Appendix A. Supplementary material

Supplementary data associated with this article can be found, in the online version, at doi:10.1016/j.reactfunctpolym.2010.11.014.

References

[1] R. Po, M. Maggini, N. Camaioni, J. Phys. Chem. C 114 (2010) 695.
[2] F. Laquai, Y. Park, J. Kim, T. Basche, Macromol. Rapid Commun. 30 (2009) 1203.
[3] T. Umeyama, T. Takamatsu, N. Tezuka, Y. Matano, Y. Araki, T. Wada, O. Yoshikawa, T. Sagawa, S. Yoshikawa, H. Imahori, J. Phys. Chem. C 113 (2009) 10798.
[4] T. Morikita, T. Yasuda, T. Yamamoto, React. Funct. Polym. 68 (2008) 1483.
[5] S. Wakim, B.R. Aich, Y. Tao, M. Leclerc, Polym. Rev. 48 (2008) 432.
[6] A. Cravino, Poym. Int. 56 (2007) 943.
[7] R. Gomez, D. Veldman, R. Blanco, C. Seoane, J.L. Segura, R.A.J. Janssen, Macromolecules 40 (2007) 2760.
[8] B.C. Thompson, Y.G. Kim, T.D. MaMarley, J.R. Reynolds, J. Am. Chem. Soc. 128 (2006) 12714.
[9] A. Iraqi, G.W. Barker, D.F. Pickup, React. Funct. Polym. 66 (2006) 195.
[10] H. Wang, Z. Li, B. Huang, Z. Jiang, Y. Liang, H. Wang, J. Qin, G. Yu, Y. Liu, Y. Song, React. Funct. Polym. 66 (2006) 993.
[11] C. Winder, N.S. Sariciftci, J. Mater. Chem. 14 (2004) 1077.
[12] I. Yamaguchi, K. Goto, M. Sato, Macromolecules 42 (2009) 7836.
[13] Y.-S. Kim, D.G. Kim, N.Y. Kwon, H.J. Kim, M.S. Choi, M. Lee, T.S. Lee, React. Funct. Polym. 70 (2010) 223.
[14] J. Choi, B. Lee, J.H. Kim, Synth. Met. 159 (2009) 1922.
[15] C.S. Wu, Y. Chen, Macromolecules 42 (2009) 3729.
[16] J.H. Kim, H.S. Lee, Synth. Met. 157 (2007) 1040.
[17] H.H. Sun, C.Y. Mei, Q.G. Zhou, Z. Lin, D.G. Ma, L.X. Wang, X.B. Jing, F.S. Wang, J. Polym. Sci. Part A Polym. Chem. 44 (2006) 3469.
[18] S.-H. Chen, Y. Chen, Macromolecules 38 (2005) 53.
[19] S. Janietz, J. Barche, A. Wedel, D. Sainova, Macromol. Chem. Phys. 205 (2004) 1916.
[20] S.-H. Chen, C.-S. Shiau, L.-R. Tsai, Y. Chen, Polymer 47 (2006) 8436.
[21] P.M. Hergenrother, Macromolecules 3 (1970) 10.
[22] M.J. Frisch, G.W. Trucks, H.B. Schlegel, G.E. Scuseria, M.A. Robb, J.R. Cheeseman, J.A. Montgomery Jr., T. Vreven, K.N. Kudin, J.C. Burant, J.M. Millam, S.S. Iyengar, J. Tomasi, V. Barone, B. Mennucci, M. Cossi, G. Scalmani, N. Rega, G.A. Petersson, H. Nakatsuji, M. Hada, M. Ehara, K. Toyota, R. Fukuda, J. Hasegawa, M. Ishida, T. Nakajima, Y. Honda, O. Kitao, H. Nakai, M. Klene, X. Li, J.E. Knox, H.P. Hratchian, J.B. Cross, C. Adamo, J. Jaramillo, R. Gomperts, R.E. Stratmann, O. Yazyev, A.J. Austin, R. Cammi, C. Pomelli, J. W. Ochterski, P.Y. Ayala, K. Morokuma, G.A. Voth, P. Salvador, J.J. Dannenberg, V.G. Zakrzewski, S. Dapprich, A.D. Daniels, M.C. Strain, O. Farkas, D.K. Malick, A.D. Rabuck, K. Raghavachari, J.B. Foresman, J.V. Ortiz, Q. Cui, A.G. Baboul, S. Clifford, J. Cioslowski, B.B. Stefanov, G. Liu, A. Liashenko, P. Piskorz, I. Komaromi, R.L. Martin, D.J. Fox, T. Keith, M.A. Al-Laham, C.Y. Peng, A. Nanayakkara, M. Challacombe, P.M. W. Gill, B. Johnson, W. Chen, M. W. Wong, C. Gonzalez, J.A. Pople, Gaussian 03, Revision A.1, Gaussian, Inc., Pittsburgh, 2003.
[23] E. Jansson, P.C. Jha, H. Agren, Chem. Phys. 330 (2006) 166.
[24] T. Yamamoto, B.-L. Lee, Macromolecules 35 (2002) 2993.
[25] T. Yasuda, Y. Sakai, S. Aramaki, T. Yamamoto, Chem. Mater. 17 (2005) 6060.
[26] T. Yamamoto, A. Mahmut, M. Abe, S. Kuroda, T. Imase, S. Sasaki, J. Polym. Sci. Part B Polym. Phys. 43 (2005) 2219.
[27] T. Yamamoto, S. Otsuka, K. Namekawa, H. Fukumoto, I. Yamaguchi, T. Fukuda, N. Asakawa, T. Yamanobe, T. Shiono, Z. Cai, Polymer 47 (2006) 6038.
[28] T. Yasuda, K. Namekawa, T. Iijima, T. Yamamoto, Polymer 48 (2007) 4375.
[29] T. Morikita, I. Yamaguchi, T. Yamamoto, Adv. Mater. 13 (2001) 1862.
[30] R.S. Ashraf, E. Klem, J. Polym. Sci. Part A Polym. Chem. 43 (2005) 6445.
[31] X. Zhang, A.S. Shetty, S.A. Jenekhe, Macromolecules 32 (1999) 7422.
[32] M. Ranger, M. Leclerc, Can. J. Chem. 76 (1998) 1571.